

CHANGING FREQUENCY SEPARATION OF KILOHERTZ QUASI-PERIODIC OSCILLATIONS IN THE SONIC-POINT BEAT-FREQUENCY MODEL

FREDERICK K. LAMB^{1,2,3} AND M. COLEMAN MILLER⁴

Received 2000 August 2; accepted 2001 January 2

ABSTRACT

We show that the sonic-point beat-frequency (SPBF) model of the pair of kilohertz quasi-periodic oscillations (QPOs) observed in neutron star X-ray binary systems predicts that the frequency separation $\Delta\nu$ between them is usually not exactly equal to the spin frequency ν_s of the star. Although the stellar spin interacts with the orbital motion of the accreting gas at the sonic radius with a frequency equal to sonic-point beat frequency, the X-ray oscillations are produced by interaction of the gas with the surface of the star, and their frequencies are therefore affected by the flow of the gas from the sonic radius to the stellar surface. For prograde disk flow near the star, $\Delta\nu$ is comparable to but usually less than ν_s , consistent with the observed values of $\Delta\nu$ and the values of ν_s inferred from oscillations during X-ray bursts. We show that the SPBF model also explains naturally the decrease in $\Delta\nu$ with increasing QPO frequencies seen in some sources and the plateau in the QPO frequency–X-ray flux correlation observed in 4U 1820–30. The model fits well the QPO frequency behavior observed in Sco X-1, 4U 1608–52, 4U 1728–34, and 4U 1820–30 ($\chi^2/\text{degrees of freedom} = 0.4\text{--}2.1$, not including systematic errors), giving masses ranging from 1.59 to 2.0 M_\odot and spin rates ranging from 279 to 364 Hz. Previous work on the model has shown that it naturally explains many other properties of the kilohertz QPOs. These include the existence of just two principal kilohertz QPOs in a given source, the approximate commensurability of the burst oscillation frequency and $\Delta\nu$, and the high frequencies, coherence, and amplitudes of these QPOs. In the SPBF model, the existence of kilohertz QPOs is an effect of strong-field general relativity. Thus, if the model is validated, observations of the kilohertz QPOs can be used not only to determine the properties of neutron stars but also to explore quantitatively general relativistic effects in the strong-field regime.

Subject headings: relativity — stars: neutron — stars: oscillations — stars: rotation — X-rays: stars

1. INTRODUCTION

Kilohertz quasi-periodic brightness oscillations (QPOs) have been discovered in the accretion-powered emission of more than 20 neutron star low-mass X-ray binaries using the *Rossi X-Ray Timing Explorer* (*RXTE*; see van der Klis 2000 for a review). These QPOs have frequencies ranging from ~ 500 up to ~ 1300 Hz, amplitudes $\sim 1\%$ – 15% rms in the 2–60 keV band of the *RXTE* Proportional Counter Array, and quality factors $Q \equiv \nu/\text{FWHM}$ as large as ~ 100 – 200 . They typically appear as two simultaneous peaks in power spectra of the X-ray brightness, at frequencies ν_1 and ν_2 ($> \nu_1$) that move together and can shift upward and downward in frequency by up to a factor of 2 within a few hundred seconds, apparently as a consequence of changes in the accretion rate. The frequencies of the kilohertz QPOs lie within the range expected for orbital motion near neutron stars and are almost certainly a strong-field general relativistic phenomenon (see Lamb, Miller, & Psaltis 1998; Miller 2001; van der Klis 2000).

In six of the kilohertz QPO sources, strong (amplitudes up to 50% rms) brightness oscillations with frequencies of hundreds of hertz have been observed during thermonu-

clear X-ray bursts. There is very strong evidence that these oscillations are produced by rotation of brighter regions of the stellar surface with the spin of the star and that the most prominent oscillation frequency is the stellar spin frequency ν_s or its first overtone (see, e.g., Strohmayer & Markwardt 1999; Miller 1999). The coherent oscillations observed in burst tails, after hot matter has spread around the star, and the antipodal brighter regions observed in 4U 1636–53 are strong evidence that these stars have dynamically important surface magnetic fields (Miller 1999), as expected on evolutionary grounds (Miller, Lamb, & Psaltis 1998b, hereafter MLP; Lorimer 2001). In the five sources where burst oscillations and two simultaneous kilohertz QPOs have both been detected with high confidence, the difference $\Delta\nu \equiv \nu_2 - \nu_1$ between the frequencies of the kilohertz QPOs is approximately equal to the burst oscillation frequency or to half this frequency (see van der Klis 2000; Chakrabarty 2000).

The properties of the kilohertz QPOs observed to date strongly indicate that the upper kilohertz QPO is an orbital frequency and that the lower one is generated by the beat of this frequency with the star's spin (Lamb et al. 1998; MLP; Miller, Lamb, & Cook 1998a): (1) The frequencies of the kilohertz QPOs are in the range expected for orbital motion near neutron stars, consistent with one being an orbital frequency. (2) The relatively small variation of $\Delta\nu$ in a given source and the approximate commensurability of $\Delta\nu$ with the stellar spin frequency inferred from burst oscillations indicates that the spin of the star is generating the frequency difference. (3) The observation of at most two strong kilohertz QPOs in any given source (van der Klis 2000; Méndez & van der Klis 2000), rather than three, indicates that only a

¹ Center for Theoretical Astrophysics, University of Illinois at Urbana-Champaign, Loomis Laboratory of Physics, 1110 West Green Street, Urbana, IL 61801-3080.

² Department of Physics, University of Illinois at Urbana-Champaign, Loomis Laboratory of Physics, 1110 West Greet Street, Urbana, IL 61801-3080.

³ Department of Astronomy, University of Illinois at Urbana-Champaign, 103 Astronomy Building, 1002 West Green Street, Urbana, IL 61801.

⁴ Department of Astronomy, University of Maryland at College Park, College Park, MD 20742-2421.

single sideband is being generated, rather than the two sidebands generated by other mechanisms. (4) In order to beat with the stellar spin, the other motion must be rotation about the center of the neutron star, indicating that the other motion is orbital motion. (5) Accretion of angular momentum ensures that the star is spinning in the same sense as the long-term average circulation of the gas in the disk, so that usually the frequency ν_2 of the upper kilohertz QPO is close to the orbital frequency ν_{orb} and the frequency ν_1 of the lower kilohertz QPO is close to the beat frequency $\nu_B \equiv \nu_{\text{orb}} - \nu_s$.

This and other evidence motivated the development of the sonic-point beat-frequency (SPBF) model (MLP). In this model ν_2 is close to the orbital frequency ν_{orb} at the sonic radius, where the flow in the disk changes from nearly circular to rapidly inspiraling, and ν_1 is close to ν_B , for prograde disk flow near the neutron star. (In the event that the disk flow near the star is temporarily retrograde relative to the star's spin, ν_1 would be close to ν_{orb} and ν_2 would be comparable to the retrograde beat frequency $\nu'_B \equiv \nu_{\text{orb}} + \nu_s$.) The transition to hypersonic radial inflow is an effect of strong-field gravity. In the SPBF model, the low-frequency QPOs seen in the Z and atoll sources are produced by the magnetospheric beat-frequency mechanism (Alpar & Shaham 1985; Lamb et al. 1985; MLP). The model explains naturally many features of the kilohertz QPOs in addition to their frequencies and frequency separation and the existence of only two principal QPOs in a given source (MLP). In the SPBF model, the kilohertz QPOs are a strong-field general relativistic effect, and they are therefore sensitive probes of the properties of the spacetime near the neutron star, including whether there is an innermost stable circular orbit (ISCO) and the gravitomagnetic torque created by the spin of the neutron star.

Careful analyses have shown that in the five sources where burst oscillations and kilohertz QPOs have both been detected with high confidence, the difference $\Delta\nu \equiv \nu_2 - \nu_1$ between the frequencies of the kilohertz QPOs is either equal to the burst oscillation frequency to within 4%–15% (4U 1702–43, Markwardt, Strohmayer, & Swank 1999; 4U 1728–34, Strohmayer et al. 1996, Méndez & van der Klis 1999; 4U 1636–53, Zhang et al. 1996, Wijnands et al. 1997, Méndez, van der Klis, & van Paradijs 1998a) or equal to one-half the burst oscillation frequency to within 0.7%–2% (KS 1731–26, Wijnands & van der Klis 1997; 4U 1608–52, Chakrabarty 2000). In some kilohertz QPO sources, $\Delta\nu$ has been observed to decrease systematically by 30–100 Hz, depending on the source, as ν_2 increases by a much larger amount (Sco X-1, van der Klis et al. 1997; 4U 1608–52, Méndez et al. 1998b; 4U 1735–44, Ford et al. 1998; 4U 1728–34, Méndez & van der Klis 1999; see also Psaltis et al. 1998). The separation frequency in 4U 1636–536 is slightly but significantly smaller than the spin frequency inferred from its burst oscillations (Méndez et al. 1998a).

Here we show that for prograde disk flow near the star, the SPBF model predicts that the inward radial velocity of the flow usually makes ν_1 slightly larger than ν_B and ν_2 slightly smaller than ν_{orb} , so that $\Delta\nu$ is comparable to but usually less than ν_s . Corrections to ν_B and ν_{orb} of $\lesssim 5\%$ are sufficient to account for the differences between $\Delta\nu$ and ν_s and the decrease of $\Delta\nu$ with increasing ν_2 described above. (For retrograde disk flow near the star, the inward radial velocity of the flow would usually make ν_2 slightly larger

than ν'_B and ν_1 slightly smaller than ν_{orb} , so that $\Delta\nu$ is comparable to but *greater* than ν_s .) The inward radial velocity of the accretion flow near the neutron star was included in the gasdynamical and radiation transport calculations reported by MLP, but the small effect of this motion on the frequencies of the kilohertz QPOs was neglected.

In § 2 we discuss the generation of the kilohertz QPOs in the SPBF model, derive general expressions for their frequencies taking into account the inward motion of the accretion flow, summarize the results of numerical simulations, and introduce the model of the gasdynamics in the SPBF model that we use here to calculate the frequencies of the kilohertz QPOs. In § 3 we show that despite its simplicity, this model fits accurately the frequency behavior observed in Sco X-1, 4U 1608–52, 4U 1728–34, and 4U 1820–30 and gives reasonable masses and spin rates for these neutron stars.

2. KILOHERTZ QUASI-PERIODIC OSCILLATIONS IN THE SONIC-POINT MODEL

Generation of kilohertz QPOs.—In the SPBF model, the kilohertz QPOs are produced by clumping of gas in the orbiting accretion flow near the star, probably caused by interaction of the accreting gas with the weak stellar magnetic field (see Ghosh & Lamb 1979; Aly & Kuipers 1990). Only clumps near the sonic radius R_{sp} , where the inward radial velocity of gas leaving the clumps becomes supersonic, contribute to the oscillations (see MLP). At low accretion rates, radiation drag removes angular momentum from the gas in the clumps, causing it to spiral inward to the stellar surface. At high enough accretion rates, the optical depth from the stellar surface is large and radiation drag is unimportant. Gas will nevertheless fall inward supersonically from clumps orbiting near the ISCO, if one exists, because gas will spiral inward supersonically from the ISCO even if it does not lose any angular momentum. In either case, the supersonic inflow is a strong-field general relativistic effect.

Where gas falling inward from clumps near R_{sp} impacts the stellar surface, it produces bright footprints that move around the star with a frequency nearly equal to the orbital frequency ν_{orb} of the clumps at R_{sp} , causing the X-ray flux seen by distant observers to oscillate as the footprint moves into and out of view. The frequency of this oscillation is usually less than the general relativistic Keplerian frequency ν_{K} , because the radially inward drift of the clumps causes the footprint to move around the star with a frequency less than ν_{orb} and the radial component of the radiation force causes ν_{orb} to be less than ν_{K} . *This oscillation is the upper kilohertz QPO; its frequency ν_2 is determined by the rate at which the azimuthal phase of the footprint advances.*

The weak magnetic field of the star funnels extra gas toward the magnetic poles, producing a broad beam of extra radiation that rotates with the star. Clumps orbiting in the prograde direction near R_{sp} move through this beam with frequency $\nu_B \equiv \nu_{\text{orb}} - \nu_s$. When a clump is illuminated by the beam, gas in it loses angular momentum to the radiation at a faster rate, so more gas falls inward, causing the luminosity of the footprint to oscillate with a frequency close to ν_B . *This oscillation is the lower kilohertz QPO; its frequency ν_1 is determined by the frequency at which the mass flux onto a footprint oscillates.*

The X-ray flux in both oscillations is generated primarily at the stellar surface, where most of the gravitational energy

is released, and hence both oscillations can have relatively high amplitudes.

Kilohertz QPO frequencies and frequency separation.—The kilohertz QPO frequencies predicted by the SPBF model for prograde disk flow near the star can be calculated as follows (we use Boyer-Lindquist coordinates for easy reference to infinity). Light travel time effects are negligible, and hence the time between two successive maxima of the mass inflow rate from a given clump is very close to the beat period $\Delta t_B \equiv 1/(v_{\text{orb}} - v_s)$. Let t_1 and $t_2 = t_1 + \Delta t_B$ be the times of successive maxima, let r_1 and r_2 and $2\pi\phi_1$ and $2\pi\phi_2$ be the radial and azimuthal coordinates of the clump at t_1 and t_2 , let Δt_1 and Δt_2 be the times required for the gas stripped from the clump at t_1 and t_2 to reach the surface of the star, and let $2\pi\Delta\phi_1$ and $2\pi\Delta\phi_2$ be the changes in the azimuthal phase of the gas released at t_1 and t_2 as it falls from the clump to the stellar surface. Then the frequencies of the lower and upper kilohertz QPOs are

$$v_1 = \frac{1}{t_2 - t_1 + (\Delta t_2 - \Delta t_1)} \quad (1)$$

and

$$v_2 = \frac{\phi_2 - \phi_1 + (\Delta\phi_2 - \Delta\phi_1)}{t_2 - t_1 + (\Delta t_2 - \Delta t_1)}. \quad (2)$$

Suppose first that the inward motion of the clumps near R_{sp} can be neglected. This is the approximation used in MLP to compute the frequencies of the kilohertz QPOs. Then the time required for gas to spiral inward from a given clump to the stellar surface and the change in the azimuthal phase of the gas during its inspiral do not depend on when the gas separated from the clump; i.e., $\Delta t_2 = \Delta t_1$ and $\Delta\phi_2 = \Delta\phi_1$. Because $\Delta t_2 = \Delta t_1$, the time between two successive maxima of the mass flow rate at the stellar surface is the same as at the clump, where it is Δt_B , and hence the frequency v_1 of the luminosity oscillation is $1/\Delta t_B = v_{\text{orb}} - v_s \equiv v_B$ (see eq. [1]). Because the rate at which the azimuthal phase of the footprint advances is the same as the rate at which the azimuthal phase of the clump advances, the rotation frequency v_2 of the footprint is $(\phi_2 - \phi_1)/(t_2 - t_1) = v_{\text{orb}}$ (see eq. [2]), and the difference between v_2 and v_1 is therefore v_s .

Now suppose that the inward motion of the clumps near R_{sp} is too large to be neglected. The distance of a given clump from the stellar surface decreases with time, and therefore the time required for gas to spiral inward from the clump to the surface steadily decreases. Hence $\Delta t_2 < \Delta t_1$. Equation (1) shows that to first order in the inward drift velocity v_{cl} of a clump, the frequency v_1 of the lower kilohertz QPO is $v_B(1 + v_{\text{cl}}\partial_r\Delta t) > v_B$; v_1 is greater than v_B because the inward motion of the clump reduces the spatial separation between successive maxima of the mass flow rate, analogous to the Doppler shift of a sound wave. Equation (2) shows that to this same order, the frequency v_2 of the upper kilohertz QPO is $v_{\text{orb}}(1 + v_{\text{cl}}\partial_r\Delta t) - v_{\text{cl}}\partial_r\Delta\phi - v_B^{-1}v_{\text{cl}}\partial_rv_{\text{orb}}$. Fully relativistic simulations of the gas flow and radiation transport similar to those presented in MLP show that the term proportional to $\partial_r\Delta\phi$ is usually the dominant correction term. This term describes the effect on v_2 of the fact that the gas falling inward from the clump winds a progressively smaller distance around the star as the clump drifts inward, because the gas falls through a smaller radial distance before colliding with the stellar

surface. Hence, v_2 is usually less than v_{orb} . In the simulations performed, the fractional decrease in v_2 is typically $\sim 50\%$ of the fractional increase in v_1 . The increase in v_1 and the decrease in v_2 make Δv less than v_s , although Δv and v_s remain comparable.

In the event that the accretion flow near the star is temporarily retrograde with respect to the star's spin, the time between two successive maxima of the mass inflow rate from a given clump would be $\Delta t'_B \equiv 1/(v_{\text{orb}} + v_s)$. Hence, if the inward motion of the clumps near R_{sp} can be neglected, $v_1 = v_{\text{orb}}$ and $v_2 = 1/\Delta t'_B = v_{\text{orb}} + v_s$. If the inward motion of the clumps near R_{sp} is too large to be neglected, our simulations indicate that v_1 would usually be less than v_{orb} . To first order in the inward velocity v_{cl} of a clump, $v_2 = v'_B(1 + v_{\text{cl}}\partial_r\Delta t) > v'_B$. Hence, for retrograde disk flow, Δv would be greater than but comparable to v_s .

Inward motion of clumps and gas.—A model of the inward drift of clumps near R_{sp} and of the infall of gas from the clumps is required in order to compute the detailed behavior of v_1 and v_2 . Here we consider a simple model that captures the basic physics of inward clump drift.

Let v_{cl} be the inward radial velocity of clumps near R_{sp} , let v_g be the characteristic initial inward radial velocity of the gas stripped from a clump, and assume that $v_{\text{cl}} \ll v_g$. Then for prograde gas flow near the star, $v_1 \approx v_B/(1 - v_{\text{cl}}/v_g)$ (see eq. [1]), because the motion near the clump contributes most to Δt . Based on the results of the numerical simulations cited above, we assume that the fractional decrease in v_2 is equal to one-half the fractional increase in v_1 . Then $v_2 \approx v_{\text{orb}}(1 - \frac{1}{2}v_{\text{cl}}/v_g)$. Our simulations indicate that the initial inward radial velocity of stripped gas is fairly insensitive to the distance of the clump from the star, and hence for simplicity we assume that v_g is independent of R_{sp} . We also assume for simplicity that v_{cl} and v_g are approximately constant during the lifetime of a clump.

The inward radial velocity of a clump with angular momentum J caused by removal of its angular momentum by a braking torque N is $v_{\text{cl}} = N/(\partial J/\partial r)$. For a clump of mass m in a nearly circular orbit in the Schwarzschild spacetime, $\partial J/\partial r = (m/2)(r - 6M)(r - 3M)^{-3/2}$, and hence

$$v_{\text{cl}}(R_{\text{sp}}) = \frac{(2/m)(R_{\text{sp}} - 3M)^{3/2}}{(R_{\text{sp}} - 6M)} N, \quad (3)$$

in units with $G = c = 1$. This expression for v_{cl} diverges at $R_{\text{sp}} = 6M$ because the inertia of the clump has been neglected. In reality, $v_{\text{cl}}(R_{\text{sp}})$ increases as R_{sp} approaches the radius of the ISCO but remains finite (see below).

There are several effects that may produce a braking torque N on orbiting clumps. Here we consider one likely possibility. R_{sp} lies inside the star's magnetosphere (MLP), where the pressure of the stellar magnetic field compresses gas clumps, isolating them from one another. We therefore assume that clumps near R_{sp} are in pressure equilibrium with the stellar magnetic field, that they interact only weakly with each other, and that N is dominated by the interaction of the clump with the stellar magnetic field (see Ghosh & Lamb 1979; Aly & Kuipers 1990; Ghosh & Lamb 1991). Then $N = \gamma\pi a^2 R_{\text{sp}} B_{\text{sp}}^2$, where γ is a dimensionless factor ~ 1 that depends on the distortion of the stellar magnetic field by the clump and the clump's shape, a is the mean radius of the clump, and B_{sp} is the magnetic field at R_{sp} . Radiation from the star is likely to maintain clumps at the local Compton temperature, which is almost independent of

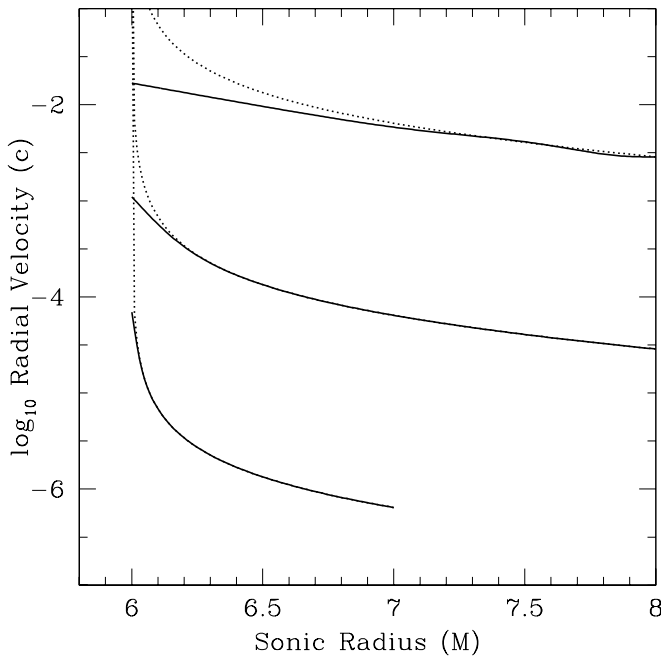


FIG. 1.—Inward radial velocity v_{cl} of clumps orbiting near the sonic radius R_{sp} as a function of R_{sp} , computed numerically (solid lines) and using eq. (3) (dotted lines), for torque coefficients $c_N = 10^{-3}$, 10^{-5} , and 10^{-7} (top to bottom) in units of the star's gravitational mass M .

the distance to the star; we therefore assume that the clump temperature is approximately independent of R_{sp} . For simplicity, we also assume that m is approximately independent of R_{sp} . Then $(3/4\pi)2mk_B T/m_p a^3 = B^2/8\pi = \mu^2 R_{sp}^{-6}$ for a dipolar field with moment μ , where m_p is the mass of a proton, and hence $a \propto R_{sp}^2$ and $N \propto R_{sp}^{-1}$.

With these assumptions, the evolution equation for the specific angular momentum u_ϕ of a clump is $du_\phi/d\tau = c_N/r$, where the torque coefficient c_N (which like u_ϕ and the proper time of the clump has the dimensions of a mass) depends on geometrical factors, fundamental constants, and γ . The evolution equation for the radial position of a clump moving in the Schwarzschild spacetime in the absence of significant nongravitational radial forces is

$$\frac{d^2 r}{d\tau^2} = -\frac{M}{r^2} + \left(1 - \frac{3M}{r}\right) \frac{u_\phi^2}{r^3}. \quad (4)$$

We computed $v_{cl}(R_{sp})$ by integrating numerically the clump equations of motion, starting with the values of \dot{r} and \ddot{r} given by equation (3) at large R_{sp} .

Figure 1 shows how v_{cl} varies with R_{sp} for $c_N = 10^{-7}$, 10^{-5} , and 10^{-3} in units of the star's gravitational mass M . These c_N values correspond to clump densities ~ 1 – 10 times the mean density in the disk, for $B_{sp} \sim 10^8$ – 10^9 G. The inward velocity of clumps increases as R_{sp} approaches the ISCO at $6M$, but remains finite. For plausible values of the torque coefficient c_N , v_{cl} is small enough even near the ISCO that the inspiral time of the clumps there is long enough to be consistent with the observed coherence of the kilohertz QPOs.

3. RESULTS AND DISCUSSION

Predictions of the model.—We have shown that contrary to statements in the literature, the kilohertz QPO frequency separation predicted by the SPBF model generally is not

exactly equal to the spin frequency of the neutron star. The fundamental reason is that in this model the X-ray oscillations are produced by interaction of accreting gas with the surface of the star. Although the beat between the spin of the star and the orbital motion of the gas occurs at the sonic-point beat frequency, the frequencies of the resulting X-ray oscillations are affected by the flow of gas from the sonic radius to the stellar surface.

We have demonstrated that for prograde disk flow near the star, the SPBF model predicts that v_1 is usually slightly greater than $v_{orb} - v_s$, that v_2 is slightly less than v_{orb} , and that Δv is therefore comparable to but usually less than v_s . In the event that the disk flow near the star is retrograde relative to the star's spin (see, e.g., Nelson et al. 1997; van Kerkwijk et al. 1998), v_1 would usually be slightly less than v_{orb} , v_2 would be slightly greater than $v_{orb} + v_s$, and Δv would therefore be comparable to but usually greater than v_s .

The fundamental frequency in the SPBF model is the orbital frequency at the sonic radius, which is typically ~ 1000 Hz. Hence, even the largest observed difference between Δv and the neutron star spin frequency inferred from burst oscillations (85 Hz, in 4U 1608–52) and the largest observed variation of Δv with accretion rate (75 Hz, also in 4U 1608–52), although highly significant, represent only very small ($\sim 5\%$) deviations of the kilohertz QPO frequencies from the values computed in the circular orbit approximation used by MLP.

Comparison with measurements.—We have compared the kilohertz QPO frequency behavior predicted by the model of inward clump drift developed in § 2 with the observed behavior of the kilohertz QPOs in four sources for which detailed frequency measurements are available.

For 4U 1608–52, the most detailed and precise measurements of the frequencies of the kilohertz QPOs have been made using the “shift-and-add” technique, which yielded a sequence of Δv versus v_1 estimates and uncertainties (Méndez et al. 1998b).⁵ The most detailed and precise measurements of kilohertz QPO frequencies in Sco X-1 (Méndez & van der Klis 2000) were also made using the shift-and-add technique, yielding a sequence of Δv versus v_2 estimates and uncertainties. The available frequency measurements for 4U 1728–34 and 4U 1820–30 are sequences of v_1 versus v_2 measurements and uncertainties.

The model of the effects of inward clump drift developed in § 2 relates the predicted frequencies of the lower and upper kilohertz QPOs, which we denote \tilde{v}_1 and \tilde{v}_2 . From these, one can compute $\Delta\tilde{v} \equiv \tilde{v}_2 - \tilde{v}_1$ versus \tilde{v}_1 and $\Delta\tilde{v}$ versus \tilde{v}_2 . We always compare the predictions of the model with the frequencies that are actually measured. Hence, for Sco X-1 we compare $\Delta\tilde{v}$ and \tilde{v}_2 with Δv and v_2 , whereas for 4U 1608–52 we compare $\Delta\tilde{v}$ and \tilde{v}_1 with Δv and v_1 . For 4U 1728–34 and 4U 1820–30 we compare \tilde{v}_1 and \tilde{v}_2 with v_1 and v_2 . For conciseness, in the discussion that follows we denote the two frequencies computed from the model for comparison with the data by \tilde{v}_a and \tilde{v}_b , regardless of which two frequencies these are.

⁵ Recently, reprocessing of the original 4U 1608–52 power spectra revealed an error in the original processing (M. Méndez 2000, private communication). When this error is corrected, the $(\Delta v, v_1)$ data points at (325.5 Hz, 472.8 Hz) and (316.9 Hz, 555.6 Hz) shown in Fig. 3 of Méndez et al. (1998b) are replaced by a single data point at $(301.3 \pm 7.9$ Hz, 506.6 ± 29.4 Hz). This latter data point was used in our fits and in constructing Fig. 2 below.

The theoretical $\tilde{\nu}_b - \tilde{\nu}_a$ relation depends on three parameters: the gravitational mass M and spin frequency ν_s of the neutron star and the coupling coefficient c_N . If M or ν_s has been determined by other considerations, the model has only two adjustable parameters. Let $\nu_{a,i}$ and $\nu_{b,i}$ denote, respectively, the i th simultaneous measurements of the two frequencies ν_a and ν_b . We assume that the errors in $\nu_{a,i}$ and $\nu_{b,i}$ are normally distributed with standard deviations $\sigma_{a,i}$ and $\sigma_{b,i}$. Suppose ν_a and ν_b are measured simultaneously n times. Then the likelihood of any given set $\{M, \nu_s, c_N\}$ of model parameters is

$$\mathcal{L}(M, \nu_s, c_N) \equiv \prod_{i=1}^n \frac{1}{2\pi\sigma_{1,i}\sigma_{2,i}} \times \exp \left[-\frac{(\nu_{b,i} - \tilde{\nu}_{b,i})^2}{2\sigma_{1,i}^2} - \frac{(\nu_{a,i} - \tilde{\nu}_{a,i})^2}{2\sigma_{2,i}^2} \right]. \quad (5)$$

Here $\tilde{\nu}_{a,i}$ and $\tilde{\nu}_{b,i}$ are the frequencies predicted by the model for the assumed values of M , ν_s , and c_N . The best-fit values of these parameters were determined by maximizing the likelihood.

We characterize the goodness of a fit by $\chi^2/\text{degrees of freedom (dof)} \equiv \hat{\chi}^2/m$, where $\hat{\chi}^2$ is twice the sum of the squared terms in the exponential in equation (5) and m is the number of degrees of freedom. For n data points ($2n$ frequencies), fits of the unconstrained model have $n + 3$ parameters (the $\tilde{\nu}_{a,i}$ plus M , ν_s , and c_N), so $m = 2n - n - 3 = n - 3$; if either M or ν_s has been determined by other considerations, then $m = n - 2$.

Figure 2 compares fits of the kilohertz QPO frequency behavior predicted by the model of the effects of inward clump drift developed in § 2 for prograde disk flow near the star to the frequency behavior observed in Sco X-1, 4U 1608–52, 4U 1728–34, and 4U 1820–30. Although we always fit to the frequencies that were measured in each source (see above), we have plotted $\Delta\nu$ versus ν_2 in Figure 2 for all four sources, for clarity and consistency. For 4U 1608–52, 4U 1728–34, and 4U 1820–30, one of the frequency estimates plotted in Figure 2 was constructed by combining two measured frequencies. The uncertainty in the derived frequency was computed by adding in quadrature the uncertainties in the frequencies that were com-

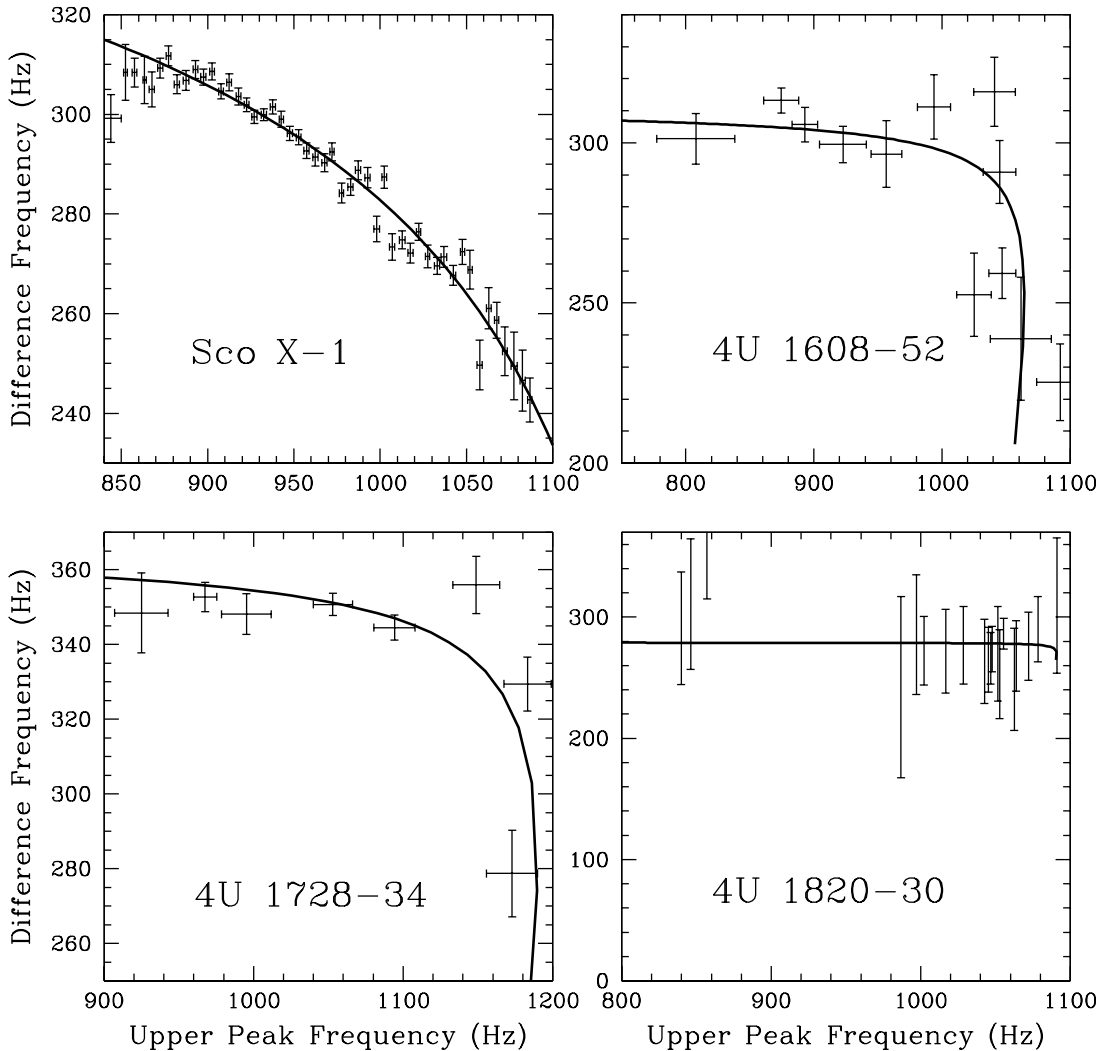


FIG. 2.—Comparison of fits of the SPBF gasdynamical model described in the text (*solid curves*) with the $\Delta\nu - \nu_2$ correlations observed in four sources. The best-fitting parameter values are Sco X-1: $M = 1.59 M_\odot$, $\nu_s = 352$ Hz, $c_N = 5 \times 10^{-3}$, $\chi^2/\text{dof} = 95.5/46$; 4U 1608–52: $M = 1.98 M_\odot$, $c_N = 3.5 \times 10^{-4}$, $\chi^2/\text{dof} = 20.6/10$; 4U 1728–34: $M = 1.745 M_\odot$, $c_N = 6 \times 10^{-4}$, $\chi^2/\text{dof} = 8.5/6$; and 4U 1820–30: $\nu_s = 279$ Hz, $c_N = 10^{-5}$, $\chi^2/\text{dof} = 7.0/18$. In the fit to the 4U 1728–34 data, ν_s was set equal to the 364 Hz frequency of the burst oscillation in this source, whereas in the fit to the 4U 1608–52 data, ν_s was set equal to half the 619 Hz frequency of the burst oscillation; in fitting the 4U 1820–30 data, M was set equal to $2.0 M_\odot$, the value indicated by the plateau in its frequency-flux relation (see text).

bined; we stress that these uncertainties were not used in the fitting procedure and are shown only to give an approximate visual impression of the goodness of the fit. The model fits well the kilohertz QPO frequency behavior in all four sources (χ^2/dof of 0.4–2.1, not including systematic errors) for masses ranging from 1.59 to 2.0 M_\odot , spin rates ranging from 279 to 364 Hz, and reasonable coupling coefficients.

Signature of the ISCO.—The refined version of the SPBF model presented here is consistent with our previous prediction (MLP) of a plateau in the kilohertz QPO frequency–X-ray luminosity correlation when the sonic radius approaches the ISCO. In particular, the fit to the 4U 1820–30 data shown in Figure 2 is consistent with the interpretation that the plateau in the QPO frequency versus X-ray flux correlation reported in this source (Zhang et al. 1998; Kaaret et al. 1999) indicates that (1) there is an ISCO around this neutron star and (2) the asymptotic frequency of the upper kilohertz QPO is the frequency of the ISCO. The indicated ISCO frequency is approximately 1100 Hz.

For the Schwarzschild spacetime used in the simple model of inward clump motion developed here, an ISCO with a frequency of 1100 Hz corresponds to a 2.0 M_\odot star (see Fig. 2). Fully general relativistic calculations of the exterior spacetimes of neutron star models rotating with the 290 Hz frequency inferred for this source (see, e.g., Miller et al. 1998a) show that the existence of an ISCO with a frequency of approximately 1100 Hz implies that the mass of the star must be approximately 2.15 M_\odot . This mass is near the maximum stable mass of stellar models with 290 Hz spin frequencies constructed using modern realistic neutron star matter equations of state (see Akmal, Pandharipande, & Ravenhall 1998). For these equations of state, the equatorial radius of a 2.15 M_\odot neutron star spinning at 290 Hz is about 10.4 km; the radius of the ISCO is about 17.8 km.

Conclusions.—We have shown that for prograde disk flow near the star, the SPBF model predicts that the inward radial motion of the accretion flow will cause the frequency separation $\Delta\nu$ between the kilohertz QPOs to be less than the spin frequency ν_s of the neutron star (for retrograde disk

flow, the model predicts that the inward radial motion of the accretion flow will cause $\Delta\nu$ to be greater than ν_s). The term $\Delta\nu$ is equal to ν_s only if the inflow velocity at the sonic radius is negligible. The inflow velocities expected at R_{sp} naturally produce the small ($\sim 0.2\%$ – 5%) corrections to the frequencies predicted for circular orbits (MLP) needed to explain the differences between $\Delta\nu$ and the spin frequency inferred from burst oscillations and the decreases of $\Delta\nu$ with increasing ν_2 observed in some sources. We have developed a simple physical model of the effect of inflow on the frequencies of the upper and lower kilohertz QPOs. The model fits well the frequencies of the kilohertz QPOs in four Z and atoll sources where they have been fairly accurately measured and gives reasonable values for the masses and spin rates of the neutron stars in these sources.

We emphasize that in the sonic-point beat-frequency model, the existence of kilohertz QPOs is an effect of strong-field general relativity. The frequencies of the kilohertz QPOs predicted by the model depend sensitively on the properties of the spacetime near the neutron star, including the gravitomagnetic torque produced by the spinning neutron star and whether there is an innermost stable circular orbit. Hence, if the sonic-point model is shown to be correct, measurements of the frequencies of the kilohertz QPOs can be used not only to determine the properties of neutron stars but also to detect and measure gravitational effects in the strong-field regime (see MLP).

We thank Michiel van der Klis, Draza Marković, Mariano Méndez, Dimitrios Psaltis, and Will Zhang for many valuable discussions. Draza Marković called our attention to the possibility of retrograde flow near the neutron star. We gratefully acknowledge the hospitality of the Aspen Institute for Physics, where many of these discussions took place. We are especially grateful to Mariano Méndez for providing the Sco X-1, 4U 1608–34, and 4U 1728–34 data and to Will Zhang for providing the 4U 1820–30 data. This research was supported in part by NSF grant AST 96-18524 and NASA grant NAG5-8424 at Illinois and NASA grant NAG5-9756 at Maryland.

REFERENCES

- Akmal, A., Pandharipande, V. R., & Ravenhall, D. G. 1998, *Phys. Rev. C*, 58, 1804
 Alpar, A., & Shaham, J. 1985, *Nature*, 316, 239
 Aly, J.-J., & Kuipers, J. 1990, *A&A*, 227, 473
 Chakrabarty, D. 2000, talk given at HEAD meeting
 Ford, E. C., van der Klis, M., van Paradijs, J., Méndez, M., Wijnands, R. A. D., & Kaaret, P. 1998, *ApJ*, 508, L155
 Ghosh, P., & Lamb, F. K. 1979, *ApJ*, 232, 259
 ———, 1991, in *Neutron Stars: Theory and Observation*, ed. J. Ventura & D. Pines (NATO ASI Ser. C, 344; Dordrecht: Kluwer), 363
 Kaaret, P., Piraino, S., Blosler, P. F., Ford, E. C., Grindlay, J. E., Santangelo, A., Smale, A. P., & Zhang, W. 1999, *ApJ*, 520, L37
 Lamb, F. K., Miller, M. C., & Psaltis, D. 1998, in *The Active X-Ray Sky*, ed. L. Scarsi, H. Bradt, P. Giommi, & F. Fiore (Amsterdam: Elsevier), 113
 Lamb, F. K., Shibazaki, N., Alpar, A., & Shaham, J. 1985, *Nature*, 317, 681
 Lorimer, D. R. 2001, in *The Neutron Star–Black Hole Connection* (NATO ASI Ser.; Dordrecht: Kluwer), in press (astro-ph/9911519)
 Markwardt, C. B., Strohmayer, T. E., & Swank, J. H. 1999, *ApJ*, 512, L125
 Méndez, M., & van der Klis, M. 1999, *ApJ*, 517, L51
 ———, 2000, *MNRAS*, 318, 938
 Méndez, M., van der Klis, M., & van Paradijs, J. 1998a, *ApJ*, 506, L117
 Méndez, M., van der Klis, M., Wijnands, R. A. D., Ford, E. C., van Paradijs, J., & Vaughan, B. A. 1998b, *ApJ*, 505, L23
 Miller, M. C. 1999, *ApJ*, 515, L77
 ———, 2001, *Astrophys. Lett. Commun.*, in press (astro-ph/0007287)
 Miller, M. C., Lamb, F. K., & Cook, G. B. 1998a, *ApJ*, 509, 793
 Miller, M. C., Lamb, F. K., & Psaltis, D. 1998b, *ApJ*, 508, 791 (MLP)
 Nelson, R. W., et al. 1997, *ApJ*, 488, L117
 Psaltis, D., et al. 1998, *ApJ*, 501, L95
 Strohmayer, T. E., & Markwardt, C. B. 1999, *ApJ*, 516, L81
 Strohmayer, T. E., Zhang, W., Swank, J. H., Smale, A., Titarchuk, L., & Day, C. 1996, *ApJ*, 469, L9
 van der Klis, M. 2000, *ARA&A*, 38, 717
 van der Klis, M., Wijnands, R. A. D., Horne, K., & Chen, W. 1997, *ApJ*, 481, L97
 van Kerkwijk, M. H., Chakrabarty, D., Pringle, J. E., & Wijers, R. A. M. J. 1998, *ApJ*, 499, L27
 Wijnands, R., et al. 1997, *ApJ*, 479, L141
 Wijnands, R., & van der Klis, M. 1997, *ApJ*, 482, L65
 Zhang, W., et al. 1996, *ApJ*, 469, L17
 Zhang, W., Smale, A. P., Strohmayer, T. E., & Swank, J. H. 1998, *ApJ*, 500, L171